Egyptian Journal of Aquatic Biology & Fisheries
Zoology Department, Faculty of Science,
Ain Shams University, Cairo, Egypt.
ISSN 1110 – 6131
Vol. 24(1): 13 – 29 (2020)
www.ejabf.journals.ekb.eg

Industrial wastewater remediation using Hematite@Chitosan nanocomposite

Abdel Halim A. Saad[1], Ahmed M. Azzam[2], Shaimaa T. El-Wakeel[3], Bayaumy B. Mostafa[2] and Mona B. Abd El-latif [2*]

1- Department of Zoology, Faculty of Science, Ain-Shams University, Cairo, Egypt.
2- Department of Environmental Researches, Theodor Bilharz Research Institute, Giza Egypt.
3- Department of Water Pollution Research, National Research Center, Egypt.

*Corresponding Author: monakhaleil@yahoo.com

ARTICLE INFO

Article History:
Received: Nov. 24, 2019
Accepted: Dec. 29, 2019
Online: Jan. 2020

Keywords:
Removal efficiency
Wastewater
Nanocomposite
Heavy metals
Hematite
Chitosan

ABSTRACT

Nowadays, the treatment of wastewater from toxic heavy metals is a long standing problem due to the industrial progress in the last years. The purpose of this study was to fabricate a novel hematite@chitosan core/organically shell nanocomposite (HCS) to remove Pb(II), Cu(II) and Cd(II) ions from industrial wastewater. The nanocomposite adsorbent was characterized by FE-SEM, TEM and FTIR resulting in formation of spherical dumb shaped particles with size range 40 to 80 nm. The effect of many operating parameters such as pH, metal ion concentration, adsorbent dosage and contact time on the removal of the toxic metal ions were investigated. The maximum removal efficacy for Pb (II), Cu (II) and Cd (II) was recorded at pH 6, 4 and 6.5, respectively. The equilibrium time was 60, 60 and 30 min, respectively while, the optimum efficiency was 94% 76% and 83% removal efficiencies for Pb (II), Cu (II) and Cd (II), respectively at initial concentration 10 mg/l. The adsorption isotherms were better matched by the Langmuir model and the metal ions adsorption capacity were 129.8, 63.2 and 69.9 mg/g, for Pb (II), Cu (II) and Cd (II), respectively. Successive adsorption-desorption cycles occur by the adsorbent confirmed that HCS NC can be reused after recovery of ions by disodium salt of EDTA solution without significant capacity loss.

INTRODUCTION

The emission of heavy metals into the environment may be natural or anthropogenic (Taghipour and Mosaferi, 2013). Anthropogenic impacts including industrial discharge, domestic sewage, non-point source runoff and atmospheric precipitation are the main sources of toxic heavy metals that enter aquatic systems (Langston *et al*., 1999). Heavy metals are bio-accumulated in living organisms when taken up and stored more than softened (metabolized) or excreted (Gupta, 2013). Heavy metals toxicity has been reportable to be caused by completely different means; e.g., from contamination of drinking-water (Pb pipes), high air concentrations close to emission sources (thus enter into soil) or from food chain. The heavy metals are poisonous as the result of the bio-accumulation (Lenntech, 2012; Gupta, 2013 & Chibuike and Obiora, 2014). The Nile in Egypt facing major environmental problems associated with the dispersal or disposal of agricultural, industrial and urban wastes generated by human activities (Abdel-Mohsien and Mahmoud, 2015).

The heavy metals in water connected most frequently to human toxicant are lead, cadmium and copper. They represent one necessary cluster of environmentally dangerous substances (Singh *et al.*, 2011b). Lead is one among the foremost known toxic metals in drinking water moreover, its higher dose than permissible limit cause general metabolic toxic and enzyme suppressor (Gebrekidan and Samuel, 2011). Cadmium is very toxicant even in low concentrations and additionally future exposures to it cause renal failure (Khan *et al.*, 2011). Copper is the necessary trace component however, high levels of it can cause brain harmful (Parveen *et al.*, 2003). Moreover, its toxicity induces iron reduction, lipid peroxidation and damage of membranes (Zaidi *et al.*, 2005).

The traditional procedures for removing heavy metal ions from aqueous streams include chemical precipitation, ion-exchange, adsorption, membrane filtration, coagulation & flocculation, flotation, reverse osmosis, solvent extraction and electrochemical treatment technologies (Fu and Wang, 2011). The adsorption method has been put on the top as one of the main methods for toxic metal separation from wastewater/ water. Because of the reversible action of most adsorption techniques, the adsorbents can be renewed by suitable desorption techniques for many use (Pan *et al.*, 2009) and multiple desorption techniques are of high efficiency, low cost and easily operated (Mishra *et al.*, 1996). Some studies discussed removal of toxic metals with cheaper and economic adsorbents (Gupta *et al.*, 2010; Gupta and Nayak, 2012& Hassan *et al.*, 2012). Modern researches proposed that several nano-sized metal oxides (NMOs) show approving sorption to toxic metals in conditions of high selectivity and capacity, which could lead to intense separation of heavy metals to face progressively strict rules (Deliyanni *et al.*, 2009). Between the useable adsorbents, NMOs, involving nano-sized ferric oxides, titanium oxides, aluminum oxides, manganese oxides, magnesium oxides and cerium oxides, which are listed as the hopeful ones for toxic heavy metals removal from liquid solutions (Agrawal and Sahu, 2006). The hematite nanoparticles (Fe_2O_3) is a magnetic NMOs which attract increasing attentions because they can be easily separated from water under a magnetic field (Mandavian and Mirrahimi, 2010). In addation, the magnetic NMOs-based composite adsorbents allowed easy isolation from aqueous solutions for recycling or regeneration after heavy metals adsorption (Zhao *et al.*, 2011). Such facile separation is essential to improve the operation efficiency and reduce the cost during water/wastewater treatment.

Chitosan is a naturally occurring polysaccharide and it has excellent properties for the adsorption of heavy metal ions, mainly due to the presence of $-NH_2$ group in chitosan matrix which mainly adsorbs metal ions in aqueous solution by ion-exchange as well as by coordination linkage (Thinh *et al.*, 2013 & Huang *et al.*, 2016). Nowadays, hybrid materials from chitosan and nanoparticles have been fabricated for toxic metals removal, which give effective adsorbent (Farzana and Meenakshi, 2015; Kandile *et al.*, 2015; Ma *et al.*, 2016& Shahzad *et al.*, 2017).

The aim of this work is to fabricate the hematite@chitosan (HCS) nanocomposite as a novel adsorbent and measuring its efficiency for removal of Pb^{2+}, Cu^{2+} and Cd^{2+} from industrial wastewater. The reusability of the HCS was evaluated by recovery and multi-cyclic reuse.

MATERIALS AND METHODS

Field Study

In this study wastewater samples were collected from three localities in three Egyptian governorates; El-Menofia (Quesna Industrial Zone, El-Khadrawia and

El-Sahl), El-Sharkia (Abbassa, Kafr El-Hosr and Bilbeis) and El-Fayium (Koum Oshim, Bahr Youssef and Bahr Hassan Wassef).

Chitosan extraction

In this work, the chitosan polymer was extracted from *Penaeus Japonicus* exoskeleton by using a procedure displayed by Abd El-Fattah *et al.* (2016). After washing of the fresh exoskeleton, it was dried under vacuum then, grinded to form powder. The powder was subjected to cycle from deproteinization, demineralization, discoloration and finally deacetylation. The technique was repeated to get high degree of deacetylation in chitosan polymer as shown in Scheme 1.

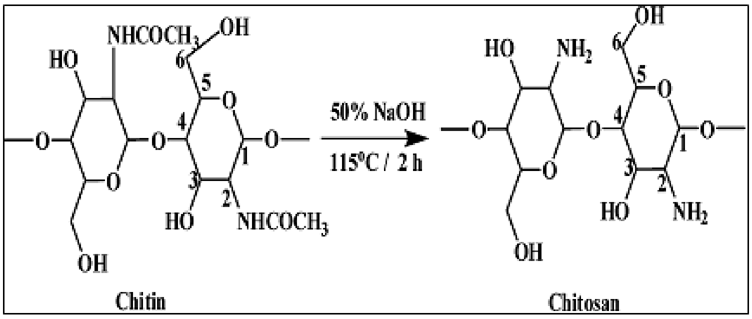

Scheme 1: Deacetylation of chitin to chitosan.

Hematite nanoparticles synthesis

Hematite nanoparticles (HNPs) was synthesized from $FeCl_3$ according to Chen and Li (2010) & Abdulkadir and Aliyu (2013) method to get a reddish brown powder from hematite nanoparticles.

Preparation of hematite@chitosan (HCS) core-shell nanocomposite

The Nanocomposite was prepared according to Cabanas-Polo *et al.*, 2015 as shown in scheme 2. To facilitate maximum coating of the hematite particles (core) with chitosan, the components were sonicated in an ultrasonic bath (Bandelin Sonorex, Germany).

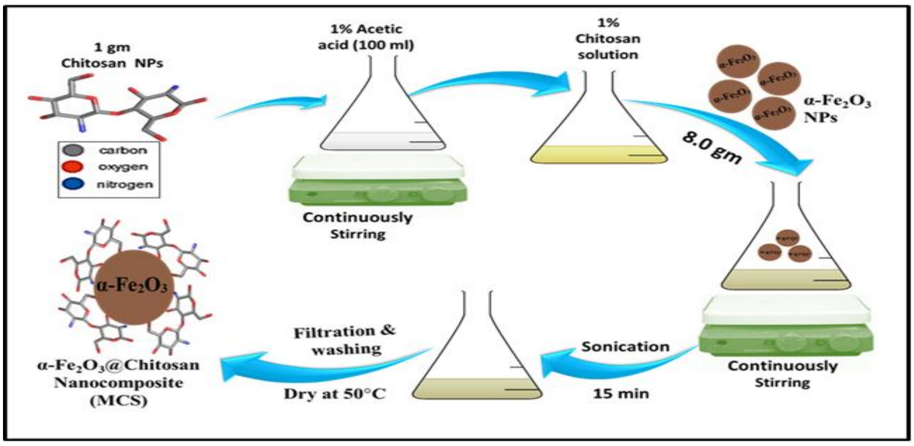

Scheme 2: Synthesis of hematite@chitosan(HCS) core-shell nanocomposite.

Hematite@chitosan nanocomposite characterization

The scanning electron microscopy (SEM), transmission electron microscope (TEM), Fourier Transform Infrared Spectroscopy (FTIR) and powder wide angel X-ray diffraction spectrometry (WAXRD) measurements were used to characterize the fabricated HCS nanocomposite. The SEM (HITACHI S-4800, Japan) and TEM (HR TEM-JEOL 2100, Japan) were used to obtain morphologies and surface homogeneity of HCS nanocomposite. The FTIR spectrum was analyzed in the spectral range 4000 – 400 cm^{-1} wave numbers on an FTIR spectrometer (Thermo Scientific Nicolet iS10 FTIR) via the KBr pressed disc method to display the functional groups of the adsorbent. The powder wide angel X-ray diffraction spectrometry (WAXRD) was performed by using Bruker D8 advance diffractometer with Cu Kα radiation in the scanning range between 5 and 80^0 2Θ (2 theta) at a scanning rate of 4^0/min.

Experimental design

In this work batch adsorption experiments were performed to study the behaviors of toxic heavy metals ions (Pb^{2+}, Cu^{2+} and Cd^{2+}) on the synthesized HCS nanocomposite. The Pb^{2+}, Cu^{2+} and Cd^{2+} sources were $PbCl_2$, $Cu_2(NO_3)_2$ and $CdCl_2$. In a typical experiment at room temperature a known amount (0.5 g/L) of the nanocomposite adsorbent was added to a synthetic solution (50 mL) of each metal ion at 20 mg/L. After that the solutions mixtures in the bottles were shaken in a rotary shaker (at 200 rpm) at different contact times. The adsorbent was removed by a 0.45 μm syringe filter and samples prepared for analysis. The concentrations of metal ions in the solution mixture were evaluated by using Inductively Coupled Plasma Optical Emission Spectroscopy (ICP-OES, Agilent 5100).

The adsorption capacity, q_e (mg/g), of metal ions and the removal efficiency at the equilibrium was calculated using following equations (Lasheen *et al.*, 2016):

$$q_e = \frac{(C_0 - C_e)V}{W} \times 100$$

$$\% \text{ Removal } = \frac{C_0 - C_e}{C_0} \times 100$$

Where, q_e is the equilibrium adsorption capacity (mg/g), C_0 and C_e are the initial and equilibrium concentrations of heavy metals ions in the solution mixture (mg/L), respectively. V is the sample volume (L) and W is the mass of HCS adsorbent used (g).

The action of different parameters such as pH, contact time, metal ion concentration and adsorbent dosage were studied to investigate the optimum adsorption efficiency. To identify the equilibrium contact time, pH, dose and initial concentration; different contact times from 5 to 120 min, pH range from 3 to 7, different HCS NC dosage (0.05, 0.1, 0.5, 0.8 and 1.0 g/L) and different initial metal ions concentrations (of Pb(II), Cu(II) and Cd (II): 10, 20, 40, 80 and 160 mg/L of each metal) were used, while the other conditions remained the same as the typical experiment.

Adsorption kinetic experiments were investigated at optimum pH and dosage of the HCS adsorbent using different contact times. To predict the adsorption kinetic model, we fitted the experimental data with the two kinetics models. The pseudo first-order equation detect adsorption in solid– liquid phase depend on the sorption capacity of solids. The pseudo-first order kinetic model (Chen and Li, 2010) is given as:

$$\log(q_e - q_t) = \log q_e - \frac{k_1 t}{2.303}$$

Where, q_e and q_t are the amounts of the heavy metal ions adsorbed on the HCS NC adsorbent in mg g^{-1} at equilibrium and at time t, respectively, while K_1 is the first-order adsorption constant in (min^{-1}).

The pseudo-second-order kinetic equation (Chen and Li, 2010) was applied to detect higher description of the kinetics is showed as:

$$\frac{1}{q_t}=\frac{1}{k_2 q_e{}^2}+\frac{t}{q_e}$$

Where, K_2 is the second-order adsorption constant in (g/mg. min).

Studying of the adsorption isotherms

In the experiments of adsorption isotherm the metals ions solutions were at diverse initial concentrations (10, 20, 40, 80, and 160 mg/L) at room temperature and using the equilibrium pH, contact time and dosage of the adsorbent. The data of the experiment were fitted in Freundlich 1906, Langmuir 1916 and Dubinin Kaganer Radushkevich (DKR) equations. The empirical Freundlich equation (Rahmani *et al.*, 2010) describes the surface heterogeneity of HCS NC adsorbent and given as:

$$\log q_e = \log k_f + \frac{1}{n}\log C_e$$

The Langmuir equation (Rahmani *et al.*, 2010) is depending on an assumption of a structurally homogeneous adsorbent, and given as:

$$\frac{C_e}{q_e}=\frac{1}{b q_{max}}+\frac{C_e}{q_{max}}$$

Where, q_e is the amount of heavy metal ions adsorbed per unit weight of adsorbent at a specified equilibrium (mg.g^{-1}), C_e is the optimum concentration of the solution (mg L^{-1}), K_F is the Freundlich constant that represent the adsorption capacity (mg/g), and n is a constant, q_{max} is the maximum adsorption at monolayer coverage (mg/g), and b is the Langmuir constant related to the energy of adsorption that quantitatively reflects the affinity of the binding sites (mg^{-1}L).

Dubinin Kaganer Radushkevich (DKR) isotherm model is used to describe adsorption on both homogeneous and heterogeneous surfaces. The general expression of the DKR isotherm (Febrianto *et al.*, 2009) can be described by:

$$In\ q = In\ q_{max} - \beta\varepsilon^2$$

Where, β is the activity coefficient related to mean sorption energy (mol^2/kJ^2), and ε is the Polanyi potential,

The value of ε can be calculated from Langmuir equation (Lasheen *et al.*, 2016) as follow:

$$\varepsilon = RT\ In\left(1+\frac{1}{C_e}\right)$$

Where, R is the ideal gas constant (8.3145 J/mol K), T is the absolute temperature (K).

Reusability of HCS nanocomposites

A solution of 20 mg/L metal ions were adsorbed using 0.5 mg of HCS NC for 60 min and after that it was desorbed with adding 10 mL of 0.01M disodium salt of ethylenediaminetetraacetic acid (Na_2EDTA) solution with continuous stirring for 60 min. The reusability was investigated by running four consecutive cycles of adsorption−desorption and the recovery efficiency, R (%), of metal ions were calculated as follows (Jiang *et al.*, 2014):

$$R(\%)=\frac{C_{des}}{C_{ads}}\times 100$$

Where, C_{des} and C_{ads} are the amount of heavy metal ions desorbed into the aqueous solution and the amount of metal ions adsorbed onto the HCS nano-adsorbents (mg/L), respectively.

Using the fabricated HCS NC in removal of metal ions from wastewater samples

Samples of wastewater were collected from three Egyptian industrials areas in El-Sharkia, El-Menofia and El-Fayium. The concentrations of three heavy metal ions (Pb(II), Cu(II) and Cd(II)) were determined before and after application of HCS NC and removal efficiency percentage was calculated. Also, coexisting ions (Na, Ca, and K) were measured in untreated and treated wastewater samples.

RESULTS AND DISCUSSION

Characteristic features of hematite@chitosan core-shell nanocomposite (HCS)

In the present study, the scanning electron microscope (SEM) picture of the hematite@chitosan nanocomposite (HCS NC) and its Bright-field image are showed in Fig.1A. Photograph studies of HCS NC by FE-SEM image revealed the hematite (α-Fe_2O_3) nanoparticles are mesocrystals characterized by a rough surface and primary crystalline domains (dumbbell-shaped) and these nanoparticles are joined together to form bundles of aggregates, which is agreed with the results of Rafi *et al.*, 2015. The composite coatings chitosan based on α-Fe_2O_3 mesocrystals are highly homogeneous coatings with well-distributed α-Fe_2O_3 particles, this result can be confirmed by results showed by Cabanas-Polo *et al.*, 2015. A spherical monodispersed α-Fe_2O_3 nanoparticles were encapsulated into the spherical dumb shaped HCS nanocomposite, which is confirmed by results discussed by Singh *et al.*, 2011a.

Fig.1B in the current study showed the transmission electron microscope (TEM) picture of the HCS NC. The particles of nanocomposites showed a rhombus-shaped form in size from 40 to 80 nm. They displayed different contrasts of α-Fe_2O_3 & chitosan, the dark color represented for crystalline α-Fe_2O_3 while the bright ones are associated with chitosan. This result of TEM image in our study is agreed and confirmed by results of Huang *et al.*, 2010, which is an evident that HCS is synthesized successfully.

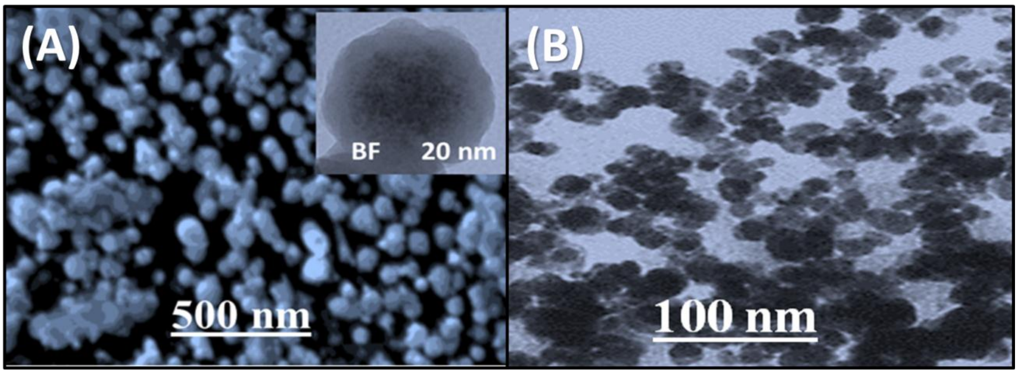

Fig. 1A: FE-SEM image and bright-field image & B) TEM images of hematite@chitosan nanocomposite.

In the current study, all the peaks which are found in pure chitosan displayed in the FTIR spectrum of the hematite @chitosan composite (Fig. 2), it is attributed to the presence of chitosan (CS) on the coating. This result confirmed by many other studies (Tian *et al.,* 2003; Beidokhti *et al.*, 2017; De Queiroz Antonino *et al.*, 2017 & Chen *et al.*, 2019). In the present study, it is important to note the small shifting of the peaks at 3411 and 1598 (1598 is due to the characteristic peak of NH_2 group in pure chitosan) cm^{-1} to 3375 and 1587 cm^{-1}, respectively. According to Singh *et al*

(2011a), this shifting of the peak around 1598 cm^{-1} indicates that the NH_2 group of CS is involved on the assembling of the α-Fe_2O_3. In the present study, the more intense bands that appear at 540 and 459 cm^{-1} in the Far-FTIR region of the α-hematite/chitosan composite coating. The appearance of these two bands supports the presence of α-Fe_2O_3 in the composite coating, which is attributed to the real success of the fabricated nanocomposite. This result agreed with Singh *et al.,* 2011a.

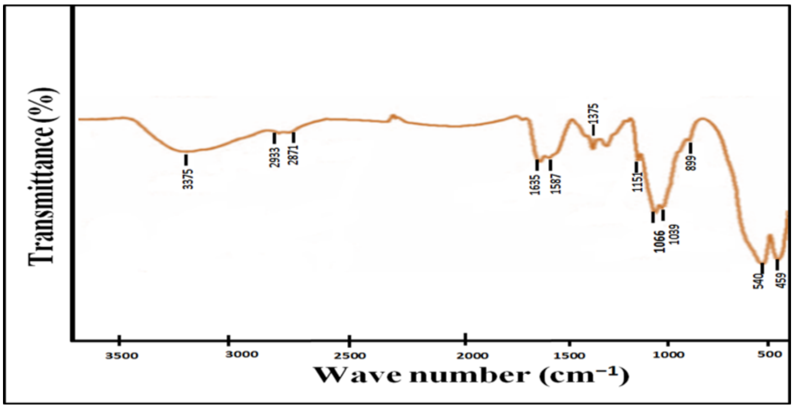

Fig. 2: FTIR spectrum of hematite@ chitosan nanocomposite.

In the present work, the X-ray powder diffraction (XRD) pattern of the HCS nanocomposite was showed in Fig.3. A small broad peak at 22.03^o was assigned to CS. The other diffraction peaks at 33.44^0, 35.94^0, 40.95^0, 49.55^0, 54.50^0, 57.50^o, 63.20^{o,} 67.50^o and 74.50^o were assigned to the (012), (104), (110), (113), (024), (116), (122), (214) and (300) planes of Fe_2O_3 respectively, which revealed that the particles crystallized in hexagonal structures. The nanocomposite coating other diffraction peaks with lower intensity can be found. The XRD peaks were in good agreement with the cubic Fe_2O_3 showing the successful formation of the hematite@chitosan nanocomposite. This result is agreed with results showed by Huang *et al.*, 2010 and Srivastava *et al.,* 2010.

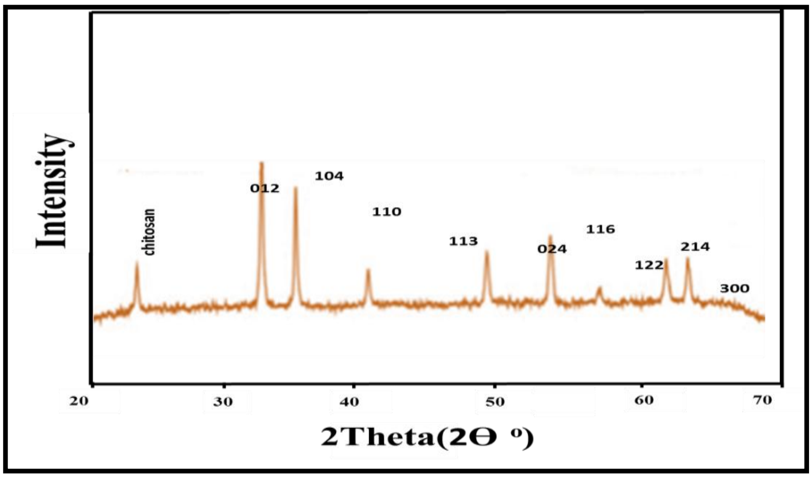

Fig. 3: The XRD pattern of hematite@chitosan nanocomposite.

Adsorption experiments

Effect of pH

In the current work, the effect of pH was investigated in the removal of heavy metal ions from aqueous solution using the synthesized HCS NC adsorbent. The pH began from 3 as chitosan may be dissolved at pH less than 3. The optimum removal efficiency for Pb(II) was 93% at pH 6 , while the optimum one for Cd (II) and Cu(II) were at pH of 6.5 and 4, respectively (Fig. 4A). The maximum removal of Cu(II) occur at pH 0.4, beyond pH 6, the precipitate was formed for Cu(II) solution, this result is supported by results showed by Sun *et al.*, 2006 & Huang *et al.*, 2012. In this result, in case of Cd(II) and Pb(II), the optimum removal occur at pH 6.5 and 6, respectively, it is clear that by increasing the pH parameter from 3 to 6 the adsorption capacity of Pb(II) and Cd(II) increases, after that decreases sharply with increasing pH. Moreover, at pH 8 and 8.5, the precipitate was formed in Cd(II) and Pb(II) solutions respectively, this is confirmed by results of Huang *et al.*, 2012. This results can be attributed to that at pH=2, low acidic medium, protonation of amino groups of chitosan (NH^{3+}) was occurred, which can lead to decrease in adsorption capacity. But, by increasing pH the competition between toxic ions cations and protons decreased and the decreasing in the positive surface charge reduces the electrostatic repulsion between surface and metal ions. This conclusion is supported by results of Liu *et al.*, 2010. The pH is an important parameter in the adsorption technique as a result of its role in the active sites of adsorbent (Liu *et al*., 2009).

Effect of contact time

The exposure time between adsorbate and adsorbent is a critical parameter in the adsorption of Cd (II), Pb(II), and Cu(II) using the prepared HCS NC (Fig. 4B). In this study, the adsorption of toxic ions increased with increasing the contact time till reached at steady state called equilibrium time. The equilibrium time was 60 min for Pb(II) and Cu(II) and 30 min for Cd(II). This result approved with Keshvardoostchokami *et al.* (2017) who used chitosan/ Fe_2O_3 nanocomposite in removal of nickel, cadmium and lead from aqueous solution. The prepared HCS NC in our study adsorbs toxic ions in the order Pb(II) > Cd(II) > Cu(II) which is in agreement with Broujeni *et al.*, 2018.

Effect of adsorbent dosage of HCS NC

One of the critical parameters that have a strong effect on the adsorption capacity is the amount of the adsorbent. Form data of the present study, the adsorption of toxic ions was highly depended on the adsorbent dose, an optimum adsorbent amount is strongly needed to magnify the interactions between toxic metal ions and active sites of adsorbent in the solution. In the current work, the maximum uptake was recorded at very low amount, keeping the other parameters such as pH, initial concentration, contact time constant, 92% of Pb(II) at 0.5 g/l, 84% of Cd(II) and 74 % of Cu(II) removed at 0.8 g/l (Fig.4C). This may be attributed to that the presence of more active sites on HCS at higher doses of adsorbent, which is confirmed by results of Laus and Fávere, 2011. From the current results, it can be concluded that, the adsorption of metals increased with increasing amount of the nanocomposite, this is agreed with result by Lasheen *et al.*, 2014. In the present experiment, the removal percentage increases as the adsorbent doses increases, but further increasing in the concentrations results in a decreasing in removal efficiency. It can be concluded that, at lower adsorbent concentrations the increasing in the adsorbent doses provides more binding sites for metal ions adsorption. However, by the increasing in adsorbent doses and no change of the agitation speed may lead to some aggregation appeared in the system, therefore less binding sites for metal ions are available at higher dose of adsorbent. This conclusion is approved with results by Zhou *et al.*, 2009.

Effect of initial metal ions concentration

In this study, the effect of initial metal concentrations ions was investigated in the range of 10-160 mg/L. The maximum removal capacities were at the lowest initial concentration of metal ions, 94%, 83% and 76% removal capacities for Pb(II), Cd(II) and Cu(II), respectively for HCS (Fig.4D). It can be concluded that the removal capacities decreased with increasing the metal ions initial concentrations. This is due to increasing the metal ions concentration but, the adsorbent active sites were not increased correspondingly .This result confirmed by Han *et al.*, 2006 and Dong *et al.*, 2017.

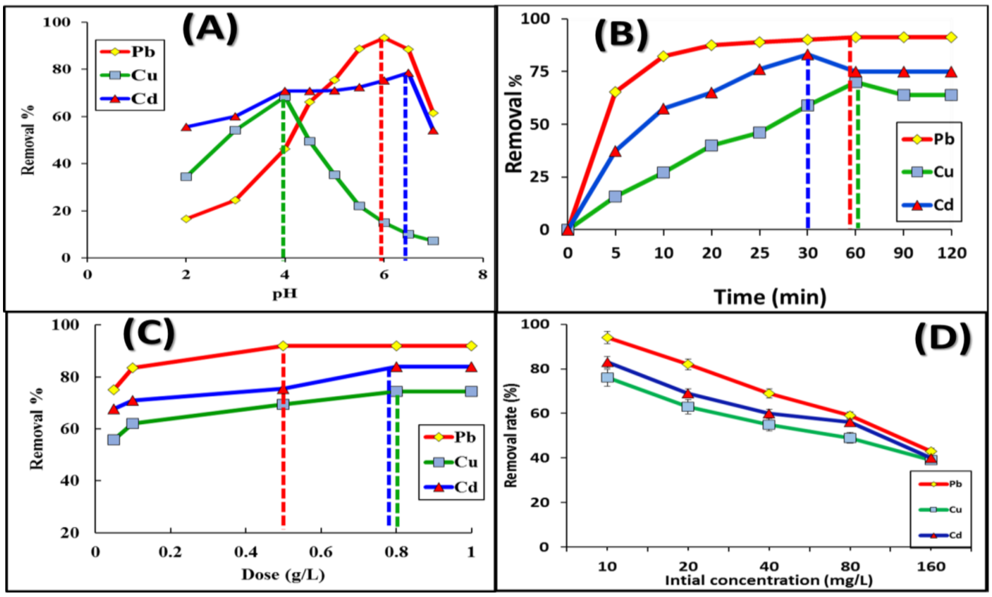

Fig. 4 A: Effect of pH; B: Effect of contact time; C) Effect of Absorbent dose, and D) Effect of initial concentration of heavy metals ions on removal rates by hematite@chitosan nanocomposite (shaking rate: 200 rpm at room temperature).

Adsorption equilibrium models

Adsorption isotherm

In the present study, Table 1, showed that the adsorptions procedure occurred on heterogeneous surfaces; assuming that many binding sites present on the adsorbent surface, which is agreed with the chemical structure of HCS NC according to Freundlich isotherm equation. Also, the current data proving highly binding chemisorption between toxic metal ions and HCS nanocomposite according to Regression coefficient (R^2) values which were achieved at 1/n values less than one, therefore the achieved high values of R^2 proved that the equilibrium data were fitting with the adsorption model (Fig. 5A). The current results is supported and agreed with Charpentier *et al.*, they pointed to type of reaction according to R^2 values (Charpentier *et al.*, 2016) and Lin *et al.*, according to n values (Lin *et al.*, 2009).

In the present study, Fig. 5B showed the calculation of the q_{max} values and b from the slope and intercept. The resulting data of Langmuir equation proved that these data were fitted to the Langmuir equation and the adsorption efficiencies of HCS nanocomposite was 129.8 > 69.9 > 63.2 mg/g for Pb(II), Cd(II), and Cu(II), respectively (Table 1). This current data according to Langmuir isotherm equation assumes the presence of monolayer of toxic ions cover out surface of the composite (physical adsorption) and there is no reaction between adsorbate and adsorbent, therefore, the saturation occurred, suggesting that the adsorbent surface has a definite number of sites of similar energy and each adsorbate ion is bind at a single finite site which is in agreement with results by Abou El Fadl, 2014. Also our results supported by Zhao *et al.* & Chen and Wang; they achieved high adsorption efficiency and the equilibrium data was applied well by Langmuir model (Zhao *et al.*, 2007& Chen and Wang, 2008).

In the present experiment, the DKR isotherm model is considered as a semi-empirical equation, by applying the data for HCS NC, the maximum adsorption capacity q_{max} (mol/g) was calculated (Fig. 5c). The values of ε for the HCS NC in the current work were 12.9, 11.9 and 10.6 kJ/mol for Pb(II), Cd(II) and Cu (II), respectively (Table 1), thus the adsorption is assumed by chemical ion-exchange. This result was agreed with result by Lasheen *et al.*, 2014.

This is attributed to that ε number is used for choose the mode of action between nanoadsorbent and metal ions during removal technique., if ε is in the range of 8–16 kJ/mol, the adsorption is assumed by chemical ion-exchange, while at ε less than 8 kJ/mol, the physical reaction represent the adsorption process (Hao *et al.*, 2010).

Table 1: Isotherm models parameters for the adsorption of Cu(II), Pb(II) and Cd(II) by HCS nanocomposite.

Freundlich isotherm parameters	**Cu(II)**	**Pb(II)**	**Cd(II)**
1/n	0.38	0.32	0.34
K_F(mg/g)	9.58	27.2	13.4
R^2	0.92	0.92	0.92
Langmauir isotherm parameters	**Cu(II)**	**Pb(II)**	**Cd(II)**
q_{max}(mg/g)	63.2	129.8	69.9
b(L/mg)	0.05	0.8	0.07
R^2	0.99	0.99	0.99
DKR isotherm parameters	**Cu(II)**	**Pb(II)**	**Cd(II)**
q_{max}(mol/g)	$2x10^{3-}$	$1.6x10^{3-}$	$1x10^{3-}$
ε (KJ/mol)	10.6	12.9	11.9
R^2	0.92	0.96	0.95

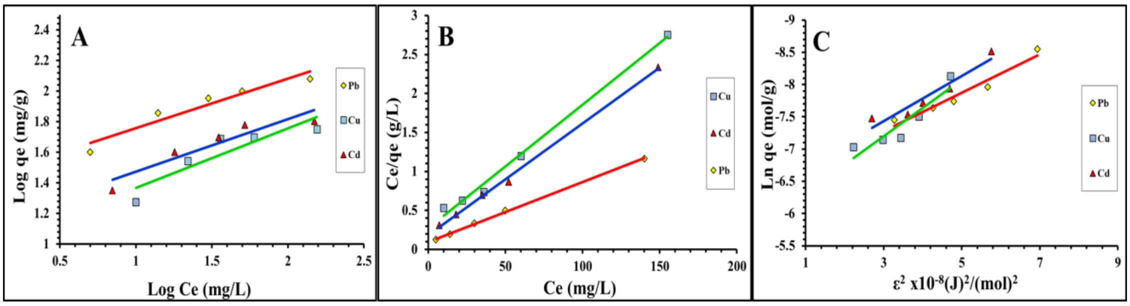

Fig. 5 A: Freundlich isotherm; B) Langmuir isotherm, and C) DKR isotherm plots for metals adsorption by HCS (absorbent dose: 0.5 g/l for Pb and 0.8 g/l for Cu and Cd; pH value: 4, 6.5, 6 for Cu, Cd and Pb respectively; initial concentration: 20 mg/L; contact time: 30–60 min, agitation time: 200 rpm).

Adsorption kinetics

In the present work, the data of first-order kinetic equation for the adsorption of metal ions (Cu^{2+},Pb^{2+} and Cd^{2+}) by HCS proved that the calculated q_e value obtained by this model don't match with the experimental value (the experimental q_e) of first-order model (Table 2 and Fig. 6) whereas, the calculated q_e values are strongly agreed with the experimental data of this equation. However, R^2 regression coefficient (correlation coefficient) of equation for the linear plots are very close to one therefore, by this way the reaction near to equilibrium and the adsorption process is chemisorption. This result was approved with the results of Shekhawat *et al.*, 2017 and highly agreed with Lasheen *et al.*, 2014 and Chen *et al.* (2019).

Table 2: Kinetic parameters for Cd (II), Pb (II) and Cu (II) adsorption by HCS nanocomposite at room temperature (adsorbent dose: 0.5 g/L, pH value: 5.5, metals concentration: 20 mg/L, contact time: 5–120 min, agitation speed: 200 rpm).

Pseudo-first order	**Cd(II)**	**Pb(II)**	**Cu(II)**
q_e (mg/g)(calculated)	40.6	75.2	36.2
q_e (mg/g)(experiment)	13	10	29
$K_1(min^{-1})$	0.1	0.09	0.05
R^2	0.88	0.90	0.92
Pseudo-second order			
q_e (mg/g)(calculated)	40.6	75.2	36.2
q_e (mg/g)(experiment)	42.3	75.7	42.7
K_2(g/mg min)	0.14	0.02	0.002
R^2	0.99	0.99	0.99

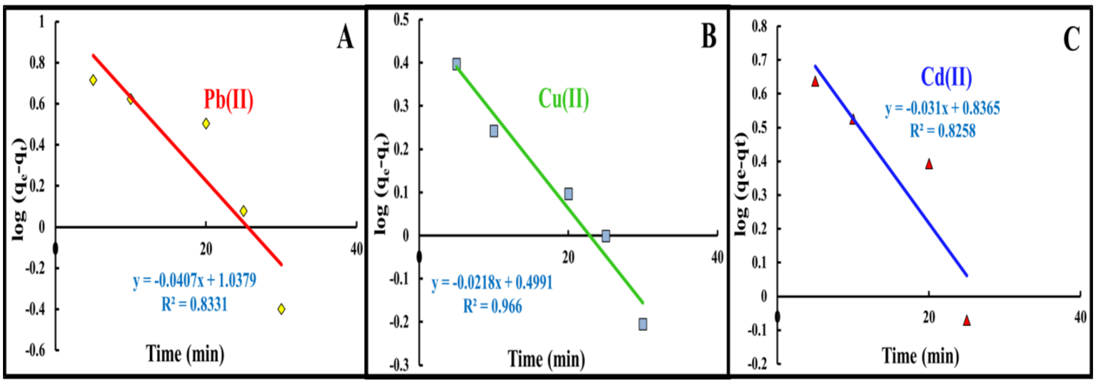

Fig. 6 A, B and C: Pseudo-first order sorption kinetics of metal ions (Pb(II), Cu(II) and Cd(II)) by HCS.

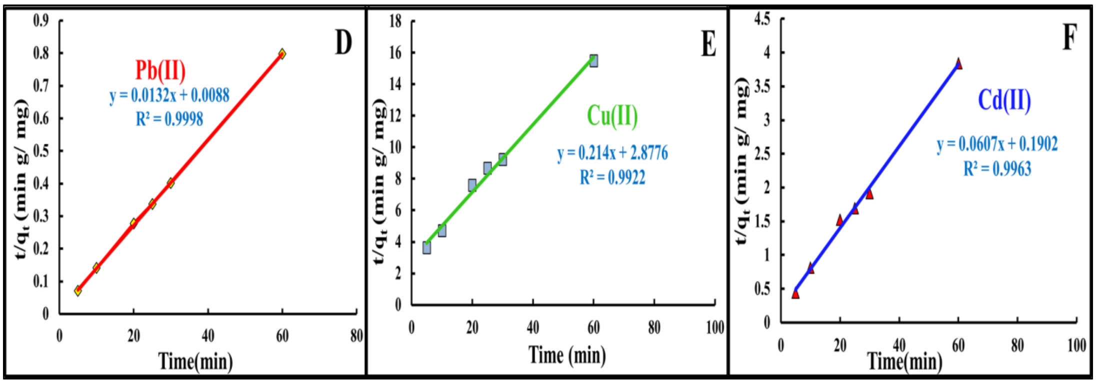

Fig. 6 D, E and F: Pseudo-second order sorption kinetics of metal ions (Pb (II), Cu (II) and Cd (II)) by HCS.

Regeneration of metal ions and recycling of HCS NC

For regeneration investigation and stability of nanoadsorbent, a number of cycles were checked. In the present work, the regeneration capacity of tested metal ions from HCS nanocomposite was investigated by using 0.01M Na_2EDTA, no observed drop in adsorption capabilities for the tested metal ions even after 4 adsorption-desorption cycles, the capacities were > 98% for Pb(II), > 94% for Cd(II) and > 91% for Cu(II). Hence the regeneration capacity of HCS for three ions was fully regenerated with significant regeneration capacity during many cycles (Fig. 7). This result is supported by result of Chen *et al.*, 2019, which the nanocomposite is almost fully regenerated.

It can be concluded that the synthesized HCS nanocomposite can act as a highly renewable and stable adsorbent for practical application and can satisfy the increasing need for the purification of water resources.

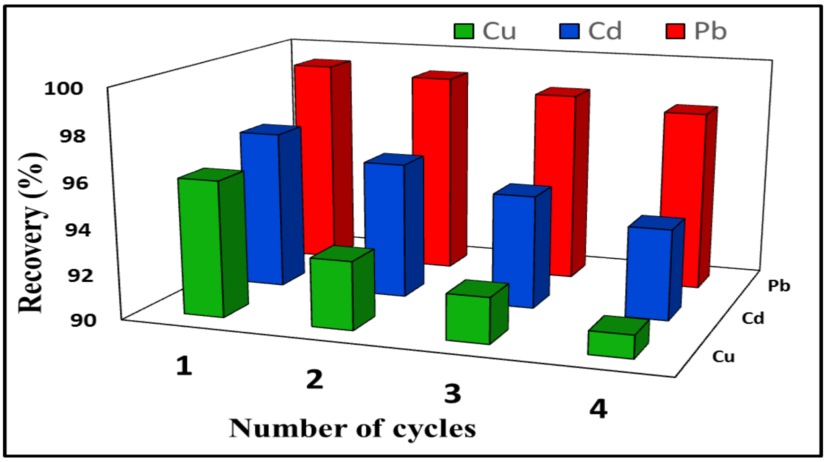

Fig. 7: Regeneration percentage of HCS nanocomposite for Pb(II), Cd(II) and Cu (II) during cyclic experiments (initial concentration of 20 mg/L at pH 4.0, 6.0 and 6.5, respectively).

Removal of metal ions from wastewater samples

In this work, nine wastewater samples, from three governorates, were treated to determine the sorption performance of the synthesized HCS adsorbent. The results were shown in Table 3. The removal rates of toxic metals from the selected samples were treated under condition of pH 5.5, 0.5 mg/L HCS NC, shaking time 1 h and room temperature. The removal rates of HCS for Pb(II), Cd(II) and Cu(II) were >96.5% for Pb (II), >95% for Cd(II) and >89.9% for Cu(II) in the presence of coexisting ions (Na, K and Ca) (Chiban *et al.*, 2016). These proved that HCS NC showed highly strong effect in environmental remediation and wastewater treatment.

Table 3: Analysis of heavy metal ions and Coexisting ions in wastewater samples with HCS nanocomposite.

Sample source	Site	Heavy metals ion (mg L^{-1})			Coexisting ions (mg L^{-1})			Removal rate (%)		
		Cu^{2+}	Pd^{2+}	Cd^{2+}	Na^{+}	K^{+}	Ca^{2+}	Cu(II)	Pd(II)	Cd(II)
El-Sharkia	S1	9.99	0.0043	0.0067	23.2	8.5	52.1	90.2	98.3	96.8
	S2	4.42	0.0054	0.0045	24.7	9.1	27.3	91.0	98.1	97.2
	S3	1.45	0.0048	0.0035	26.1	8.9	27.0	90.5	98.5	96.5
El-Fayium	F1	4.45	0.098	0.0042	30.4	9.4	42.5	89.5	98.7	96.2
	F2	2.55	0.0054	0.0023	32.2	8.5	33.1	90.2	98.3	97.4
	F3	1.68	0.0151	0.0021	25.2	10.1	26.5	91.2	97.2	97.8
El-Monofia	M1	4.57	12.7	1.11	101.5	38	63.5	89.6	96.5	95.0
	M2	4.42	3.02	1.61	111.2	44	59.6	89.9	97.1	97.0
	M3	1.25	0.051	0.015	37.5	10.5	29.1	91.2	96.5	96.8

S1:Sharkia site 1, S2: Sharkia site 2, S3: Sharkia site 3, M1: Menofia site 1, M2: Menofia site 2, M3: Menofia site 3, F1: Fayium site 1, F2: Fayium site 2, F3: Fayium site 3.

CONCLUSION

In this study, hematite@chitosan core/organically shell nanocomposite (HCS) was synthesized. It is a novel, recyclable, chemically and thermodynamically stable, low cost, environmentally-friendly material, low biological toxicity, biodegradable and safe adsorbent. This adsorbent was used in Pb^{2+}, Cd^{2+} and Cu^{2+} removal from industrial wastewater many times with high regeneration capacity and stability.

RECOMMENDATION

It is recommended to use the fabricated HCS nanocomposite in heavy metals removal from industrial wastewater especially for Pb^{2+}, Cd^{2+} and Cu^{2+} metal ions.

REFERENCES

Abd El-Fattah, M.; El Saeed, A. M.; Azzam, A. M.; Abdul-Raheim, A. M. and Hefni, H. H. H. (2016). Improvement of corrosion resistance, antimicrobial activity, mechanical and chemical properties of epoxy coating by loading chitosan as a natural renewable resource. Prog. Organ. Coat., 101: 288.

Abdel-Mohsien, H. S. and Mahmoud, M. A. M. (2015). Accumulation of Some Heavy Metals in *Oreochromis niloticus* from the Nile in Egypt: Potential Hazards to Fish and Consumers. J. Environ. Protection, 6:1003-1013.

Abdulkadir, I. and Aliyu, A. B. (2013). Some wet routes for synthesis of hematite nanostructures. African Journal of Pure and Applied Chemistry, 7(3): 114-121.

Abou El Fadl, F. I. (2014). Radiation grafting of ionically crosslinked alginate/chitosan beads with acrylic acid for lead sorption. J. Radioanal. Nucl. Chem., 301: 529−535.

Agrawal, A. and Sahu, K. K. (2006). Kinetic and isotherm studies of cadmium adsorption on manganese nodule residue. J. Hazard. Mater., 137: 915–924.

Beidokhti, H. R. N.; Ghaffarzadegan, R.; Mirzakhanlouei, S.; Ghazizadeh, L. and Dorkoosh, F. A. (2017). Preparation, Characterization, and Optimization of Folic Acid-Chitosan-Methotrexate Core-Shell Nanoparticles by Box-Behnken Design for Tumor-Targeted Drug Delivery. AAPS Pharm. Sci. Tech., 18: 115.

Broujeni, B. R.; Nilchi, A.; Hassani, A. H. and Saberi, R. (2018). Preparation and characterization of chitosan/Fe_2O_3 nano composite for the adsorption of thorium (IV) ion from aqueous solution. Water Science & Technology, 78 (3): 708-720.

Cabanas-Polo, S.; Distaso, M.; Peukert, W. and Boccaccini, A. R. (2015). Electrophoretic Deposition of α-Fe_2O_3/Chitosan Nanocomposite Coatings for Functional and Biomedical Applications. Journal of Nanoscience and Nanotechnology, 15:10149–10155.

Charpentier, T. V. J.; Neville, A.; Lanigan, J. L.; Barker, R.; Smith, M. J.; Richardson, T. (2016). Preparation of Magnetic Carboxymethylchitosan Nanoparticles for Adsorption of Heavy Metal Ions. ACS Omega, 1(1): 77-83.

Chen, B.; Zhao, H.; Chen, S.; Long, F.; Huang, B.; Yang, B. and Pan, X. (2019). A magnetically recyclable chitosan composite adsorbent functionalized with EDTA for simultaneous capture of anionic dye and heavy metals in complex wastewater. Chemical Engineering Journal, 356: 69–80.

Chen, C. and Wang, J. L. (2008). Removal of Pb^{2+}, Ag, Cs and Sr^{2+} from aqueous solution by brewery's waste biomass. J. Hazard. Mater., 151: 65-70.

Chen, Y. H. and Li, F. A. (2010). Kinetic study on removal of copper(II) using goethite and hematite nano-photocatalysts. J. Colloid. Interf. Sci., 347: 277-281.

Chiban, M.; Carja, G.; Lehutu, G. and Sinan, F. (2016). Equilibrium and thermodynamic studies for the removal of As(V) ions from aqueous solution using dried plants as adsorbents. Arab J. Chem., 9: 5988-5999.

Chibuike, G. U. and Obiora, S. C. (2014). Heavy metal polluted soils: Effect on plants and bioremediation methods. Applied and Environmental Soil Science., 2014: 1-12.

De Queiroz Antonino, R. S. C. M.; Lia Fook , B. R. P.; de Oliveira Lima, V. A.; De Farias Rached, R. Í.; Lima , E. P. N.; Da Silva Lima , R. J.; Peniche Covas, C. A. and Lia Fook, M. V. (2017). Preparation and Characterization of Chitosan Obtained from Shells of Shrimp (Litopenaeus vannamei Boone). Mar Drugs., 15(5): 141-152.

Deliyanni , E. A.; Peleka, E. N. and Matis, K. A. (2009). Modeling the sorption of metal ions from aqueous solution by iron-based adsorbents. J. Hazard Mater., 172: 550–558.

Dong, L.; Wen, C.; Junxia, Y. and Yigang, D. (2017). Polyamine chitosan adsorbent for the enhanced adsorption of anionic dyes from water. Water Sci. Technol., 18:1832-1841.

Farzana, M. H. and Meenakshi, S. (2015). Photocatalytic aptitude of titanium dioxide impregnated chitosan beads for the reduction of Cr(VI). International Journal of Biological Macromolecules, 72: 1265-1271.

Febrianto, J.; Kosasih, A. N.; Sunarso, J.; Ju, Y. H.; Indraswati, N.; Ismadji, S. (2009). Equilibrium and kinetic studies in adsorption of heavy metals using biosorbent: asummary of recent studies. J. Hazard. Mater., 162: 616–645.

Freundlich, H. M. F. (1906). Uber Die Adsorption in Lasungen. Journal of Physical Chemistry, 57: 385-370.

Fu, F. and Wang, Q. (2011). Removal of heavy metal ions from wastewaters: A review. Journal of Environmental Management, 92: 407-418.

Gebrekidan, M. and Samuel, Z. (2011). Concentration of Heavy Metals in Drinking Water from Urban Areas of the Tigray Region, Northern Ethiopia. MEJS, 3(1):105-121.

Gupta, V. (2013). Mammalian Feces as Bio-Indicator of Heavy Metal Contamination in Bikaner Zoological Garden, Rajasthan, India. Res. J. Animal, Veterinary and Fishery Sci., 1(5): 10-15.

Gupta, V. K. and Nayak, A. (2012). Cadmium removal and recovery from aqueous solutions by novel adsorbents prepared from orange peel and Fe_2O_3 nanoparticles. Chemical Engineering Journal, 180: 81-90.

Gupta, V. K.; Rastogi, A. and Nayak, A. (2010), Adsorption studies on the removal of hexavalent chromium from aqueous solution using a low cost fertilizer industry waste material. Journal of Colloid and Interface Science, 342: 135-141.

Han, D. Y.; Jiang, X and Xie, C. S. (2006). Preparation and adsorption property for metal ions of crosslinked chitosan magnetic microspheres. Environ. Chem., 25: 748–751.

Hao, Y. M.; Chen, M. and Hu, Z. B. (2010). Effective removal of Cu (II) ions from aqueous solution by amino-functionalized magnetic nanoparticles. J. Hazard Mater., 184: 392-399.

Hassan, H. E.; Abdel Rahman ,A. A.; El-Sherbini, E. A.; Tawfic, T. A. and Abdel Tawab, A. R. (2012). Phytoremediation of Industrial Wastewater Polluted with Heavy Metals Using Water Hyacinth Roots. Journal of Applied Sciences Research, 8(8): 3878-3886.

Huang, C. L.; Zhang, H. Y.; Sun, Z. Y. and Liu, Z. M. (2010). Chitosan-mediated synthesis of mesoporous α-Fe_2O_3 nanoparticles and their applications in catalyzing selective oxidation of cyclohexane. Sci. China Chem., 53(7): 1502–1508.

Huang, J.; Ye, M.; Qu, Y.; Chu, L.; Chen, R.; He, Q. and Xu, D.(2012). Pb (II) removal from aqueous media by EDTA-modified mesoporous silica SBA-15. J. Colloid Interface Sci., 385: 137–146.

Huang, K. S.; Yang, C. H.; Huang, S. L.; Chen, C. U.; Lu, Y. Y. and Lin, Y. S. (2016). Recent Advances in Antimicrobial Polymers: A Mini-Review. Int. J. Mol. Sci., 17(9): 1578-1591.

Jiang, Y.; Wang, W. N.; Biswas, P. and Fortner, J. D. (2014). Facile Aerosol Synthesis and Characterization of Ternary Crumpled Graphene–TiO_2–Magnetite Nanocomposites for Advanced Water Treatment. ACS Appl. Mater. Interface, 6(4): 11766-11774.

Kandile, N. G.; Mohamed, H. M. and Mohamed, M. I. (2015). New heterocycle modified chitosan adsorbent for metal ions (II) removal from aqueous systems. International Journal of Biological Macromolecules, 72: 110-116.

Keshvardoostchokami, M.; Babaei, L.; Zamani, A. A.; Parizanganeh, A. H. and Piri, F. (2017). Synthesized chitosan/ iron oxide nanocomposite and shrimp shell in removal of nickel, cadmium and lead from aqueous solution. Global J. Environ. Sci. Manage., 3(3): 267-278.

Khan, S. A.; Din, Z. U.; Ihsanullah and Zubair, A. (2011). Levels of selected heavy metals in drinking water of Peshawar city. I.J.S.N., 2(3): 648-652.

Langmuir, I. (1916). The Constitution and Fundamental Properties of Solids and Liquids. Part I. Solids. Journal of the American Chemical Society, 38: 2221-2295.

Langston, W. J.; Burt, G. R. and Pope, N. D. (1999). Bioavailability of metals in sediments of the dogger bank (Central North Sea): A mesocosm study. Estuarine. Coastal and Shelf Science, 48: 519-540.

Lasheen, M. R.; El-Sherif, I. Y.; Sabry, D. Y.; El-Wakeel, S. T. and El-Shahat, M. F. (2014). Removal and recovery of Cr(VI) by magnetite nanoparticle. Desalin. Water Treat., 52: 6464–6473.

Lasheen, M. R.; El-Sherif, I. Y.; Tawfik, M. E.; El-Wakeel, S. T.; El-Shahat, M. F. (2016). Preparation and adsorption properties of nano magnetite chitosan films for heavy metal ions from aqueous solution. Materials Research Bulletin, 80: 344–350.

Laus, R. and De Fávere, V. T. (2011). Competitive adsorption of Cu (II) and Cd (II) ions by chitosan crosslinked with epichlorohydrin–triphosphate - Bioresource. Technol., 102: 8769.

Lenntech, B. V. (2012). Heavy Metals, Available at Website: www.lenntech.co./periodic.periodic-chart.htm

Lin, K.; Pan, J.; Chen, Y.; Cheng, R. and Xu, X. (2009). Study the adsorption of phenol from aqueous solution on hydroxyapatite nanopowders. J. Hazard. Mater., 161: 231−240.

Liu, Y.; Cao, X.; Hua, R.; Wang, Y.; Liu, Y.; Pang, C. and Wang, Y.(2010). Entrapment of nanoscale zero-valent iron in chitosan beads for hexavalent chromium removal from wastewater. Journal of Hazardous Materials, 184: 724-730.

Liu, X. W.; Hu, Q. Y.; Fang, Z.; Zhang, X. J. and Zhang, B. B. (2009). Magnetic Chitosan Nanocomposites: A Useful Recyclable Tool for Heavy Metal Ion Removal. Langmuir, 25: 3.

Ma, X. F.; Zhang, B.; Cong, Q.; He, X. C.; Gao, M. J. and Li, G. (2016). Improved multi-shot diffusion imaging using GRAPPA with a compact kernel. Mater. Chem. Phys., 178: 88.

Mandavian, A. R. and Mirrahimi, M. A. S. (2010). Efficient separation of heavy metal cations by anchoring polyacrylic acid on superparamagnetic magnetite nanoparticles through surface modification. Chem. Eng. J., 159: 264–271.

Mishra, S. P.; Singh, V. K. and Tiwari, D. (1996). Radiotracer technique in adsorption study: Part XIV. Efficient removal of mercury from aqueous solutions by hydrous zirconium oxide. Applied Radiation and Isotopes, 15: 21.

Pan, B.; Pan, B.; Zhang, W.; Lv, L.; Zhang, Q. and Zheng, S. (2009). Development of polymeric and polymer-based hybrid adsorbents for pollutants removal from waters. Chemical Engineering Journal, 151: 19-29.

Parveen, Z.; Khuhro, M. I. and Rafiq, N. (2003). Market basket survey for lead, cadmium, copper, chromium, nickel and zinc in fruits and vegetables. Bulletin of Environmental Toxicology, 71: 1260-1264.

Rahmani, A; Mosavi, H. Z. and Fazli, M (2010). Effect of nanostructure alumina on adsorption of heavy metals. Desalination, 253: 94–100.

Rafi, M. M.; Ahmed, K. S. Z.; Nazeer, K. P.; Kumar, D. S. and Thamilselvan, M. (2015). Synthesis, characterization and magnetic properties of hematite (a-Fe_2O_3) nanoparticles on polysaccharide templates and their antibacterial activity. Appl Nanosci, 5:515–520.

Shahzad, A.; Miran, W.; Rasool, K.; Nawaz, M.; Jang, J.; Lim, S. R. and Lee, D. S. (2017). Heavy metals removal by EDTA-functionalizedchitosan graphene oxide nanocomposites. RSC Adv., 7: 9764-9771.

Shekhawat, A.; Kahu, S.; Saravanan, D. and Jugade, R. (2017). Removal of Cd(II) and Hg(II) from effluents by ionic solid impregnated chitosan. Int. J. Biol. Macromol. 104: 1556-1568.

Singh, J.; Srivastavab, M.; Duttac, J. and Dutta, P. K. (2011a). Preparation and properties of hybrid monodispersed magnetic α-Fe_2O_3 based chitosan nanocomposite film for industrial and biomedical applications. International Journal of Biological Macromolecules, 48: 170–176.

Singh, S.; Lal, S.; Harjit, J.; Amlathe, S. and Kataria, H. C. (2011b). Potential of Metal Extractants in Determination of Trace Metals in Water Sample. Advanced Studies in Biology, 3(5): 239-246.

Srivastava, M.; Ojha, A. K.; Chaubey, S.; Singh, J.; Sharma, K. P.; Pandey, C. A. and Alloys, J. (2010). Investigation on magnetic properties of nanoparticles synthesized under surfactant-free condition by hydrothermal process. Compd., 500:206–210.

Sun, J. M.; Zhu, W. T. and Huang, J. C. (2006). Characterization of primary precipitate composition formed during co-removal of Cr (VI) with Cu (II) in synthetic wastewater. Environ. Sci. Pollut. Res. Int., 13: 379.

Taghipour, H. and Mosaferi, M. (2013). Heavy metals in the vegetables collected from production sites. Health Promot Perspect. , 3(2): 185-93.

Thinh, N. N.; Hanh, P. T. B; Ha, L. T. T; Anh, L. N; Hoang, T. V. ; Hoang, V. D; Khoi, N. V. and Lam, T. D. (2013). Magnetic Chitosan Nanoparticles for Removal of Cr(VI) from Aqueous Solution, Material Science and Engineering., 33: 1214-1218.

Tian, H.; Zhang, Q.; Li, H. and Zhang, G. (2003). Antioxidant N-acetylcysteine and AMPA/KA receptor antagonist DNQX inhibited mixed lineage kinase-3 activation following cerebral ischemia in rat hippocampus. Neuroscience Research, 47: 47-53.

Zaidi, M. I; Asrar, A.; Mansoor, A. and Farooqui, M. A. (2005). The heavy metal concentrations along Road side trees of Quetta and its effects on public health. Journal of Applied Science, 5: 708-711.

Zhao, F.; Yu, B., Yue, Z.; Wang, T.; Wen, X.; Liu, Z. and Zhao, C. (2007). Preparation of porous chitosan gel beads for copper (II) ion adsorption. J. Hazard. Mater., 147: 67-73.

Zhou, Y. T.; Nie, H. L.; Branford-White, C.; He, Z. Y. and Zhu, L. M. (2009). Removal of Cu^{2+} from aqueous solution by chitosan-coated magnetic nanoparticles modified with α-ketoglutaric acid. Journal of Colloid and Interface Science, 330: 29–37.

Zhao, G.; Wu, X.; Tan, X. and Wang, X. (2011). Sorption of heavy metal ions from aqueous solutions: A review. Open Colloid Sci. J., 4:19-31.

ARABIC SUMMARY

تنقية مياه الصرف الصناعى بإستخدام مركب هيماتيت/كيتوزان النانومترى

عبدالحليم عبده سعد[1]، أحمد محمد عزام [٢]، شيماء طه الوكيل [٣] ، بيومى بيومى مصطفى [٢]
منى بشير عبداللطيف[٢]

١- قسم علم الحيوان- كلية العلوم- جامعة عين شمس – مصر.
٢- قسم بحوث البيئة- معهد تيودور بلهارس للأبحاث- امبابة – جيزة- صندوق بريد رقد ١٢٤١١- مصر.
٣- قسم أبحاث تلوث المياه- المركز القومى للبحوث- مصر.

تهدف هذه الدراسة لتصنيع مركب نانومترى جديد هو الهيماتيت مع الكيتوزان كمركب عضوى متناهى الصغر لإزالة أيونات عناصر الرصاص والنحاس والكادميوم من مياه الصرف الصناعى. تم توصيف هذا المركب النانومترى بواسطة المجهر الالكترونى الماسح والمجهر الالكترونى النافذ و طيف الاشعة تحت الحمراء. وأظهرت نتائج التوصيف للمركب تكوين جزيئات كروية يتراوح حجمها من ٤٠ الى ٨٠ نانومتر. كما تم دراسة تأثير الأس الهيدروجيني ، تركيز أيون العناصر ، جرعة المركب النانومترى، الوقت اللازم لإزالة أيونات العناصر السامة. حيث اوضحت النتائج تسجيل الإزالة القصوى لعناصر الرصاص والنحاس والكادميوم عند الأس الهيدروجيني ٦ و ٤ و ٦.٥ على الترتيب . وكان الوقت المثالى عند ٦٠ و ٦٠ و ٣٠ دقيقة للعناصر المذكورةعلى الترتيب بينما كانت افضل كفاءة إمتصاص ٩٦% و ٧٦% و ٨٣% عند تركيز ايونى ١٠ مليجرام/لتر للعناصر الثلاثة بنفس الترتيب. و تم وصف درجة حرارة متساوي الإمتصاص وكانت مطابقة بشكل أفضل لنموذج Langmuir وكانت كفاءة الإمتصاص لأيونات العناصر ١٢٩.٨ و ٦٣.٢ و ٦٩.٩ لعناصر الرصاص والنحاس والكادميوم على الترتيب . كما أوضحت النتائج قدرة المركب النانومترى على إعادة الإستخدام مرات عديدة بدون فقد القدرة على إمتصاص العناصر السامة بعد معالجته لاإزالة العناصر بإستخدام ملح ثنائى الصوديوم من محلول EDTA .